

PULSATING AURORAE AND INFRASONIC WAVES
IN THE POLAR ATMOSPHERE

Kaichi Maeda
Goddard Space Flight Center
Greenbelt, Maryland*

and

Tomiya Watanabe (*Brit. Columbia U.*)
Institute of Earth Sciences
University of British Columbia**
Vancouver, Canada

INTRODUCTION

The purpose of this paper is to interpret the origin of the strange travelling atmospheric waves observed at the ground during intervals of high geomagnetic activity (Chrzanowski, et al., 1961). In particular, we seek possible modes of atmospheric oscillations caused by the periodic bombardment of auroral particles in the polar mesosphere.

Trains of these waves are detected by a system of four microphones placed on each corner of a quadrant roughly 8 km square, located north of Washington, D.C. The presence of a travelling wave was established when the same wave forms could be found on all four records under certain time shifts among them. These time displacements were used

*This work was performed under a National Academy of Sciences post-doctoral resident research associateship, and also supported partly by the Office of Naval Research under (Contract number 3116(00))**.

FACILITY FORM 602

| | |
|---|------------------|
| <u>N65-88858</u> (ACCESSION NUMBER) | _____ (THRU) |
| <u>58</u> (PAGES) | _____ (CODE) |
| <u>TMX-57431</u> (NASA CR OR TMX OR AD NUMBER) | _____ (CATEGORY) |


58p

X63 15801

Code 2 A
15801

ABSTRACT

Pulsating aurorae are proposed as a source of the infrasonic waves associated with geomagnetic activity reported by Chrzanowski et al. One of the most plausible generation mechanism of these long period pressure waves is the periodic heating of the upper air around 100 km level, corresponding to the auroral coruscation reported by Campbell and Pees. To see the energetic relation between source input and pressure change at sea level, some theoretical calculations are performed using a simple model of auroral distribution in the isothermal atmosphere.



to determine the direction of wave propagation and the horizontal phase velocity of the waves. The periods of these infrasonic waves are usually from 20 to 80 sec, and very occasionally 100- to 300-sec waves are recorded. The pressure amplitude ranges from about one to ten dynes/cm².

One of the peculiar features of these waves is the change of arrival direction with time of day. The general trend is as follows:

They come from the northeast direction in the evening, through north about midnight, then northwest in the morning. The shift back to northeast during the following day is somewhat discontinuous. These travelling pressure waves occur less frequently in daytime.

Since auroral activity predominates around midnight local time, the time dependence of the appearance of infrasonic waves during intervals of high geomagnetic activity can be explained by assuming that the source of this kind of wave is located somewhere in the auroral region, as can be seen from Fig. 1. (Fukushima, 1960). The left side of this figure shows the diurnal variation of arrival of sound waves during magnetic storms, reported by Chrzanowski, et al. (1960).

In attempting to understand these peculiar pressure waves, we propose that they originate from a certain domain of the auroral activity, which is heated up periodically by the severe periodic bombardment of auroral particles. As we shall show later, this periodic precipitation of auroral particles is expected to take place simultaneously with the occurrence of geomagnetic pulsations.

2. Inter-relations between Geomagnetic Fluctuations, Pulsating Aurorae and Infrasonic Waves.

The auroral luminosity often fluctuates with the fluctuation of incoming auroral particles. The fluctuations of incoming particles, which are mostly electrons, can be explained either by a periodic change in the acceleration mechanism of incident particles or by the change of mirror heights of trapped particles in the earth's atmosphere, following the variations of field intensity of the earth's magnetosphere. The variations of geomagnetic field intensity and of auroral brightness are therefore closely related. A clear example of this correspondence between the pulsating aurorae and the rapid variation of geomagnetic intensity observed at the ground was given by Campbell (1960).

According to the analysis of the space-probe data given by Sonnet et al. (1960), and recently that of Explorer X given by Heppner et al. (1961, 1963), the region beyond around ten earth radii near the geomagnetic equator is occasionally greatly disturbed. Such disturbances may be propagated along the magnetic lines of force as hydromagnetic waves, and are transformed into electromagnetic waves when they reach the conducting ionosphere (Watanabe 1957, 1962, Piddington 1958). After penetrating the ionospheric region as electromagnetic waves, they will be almost perfectly reflected at the earth's surface (Sholte and Veldkamp 1955). This will produce standing hydromagnetic waves along magnetic lines of force. The simplest mode of such standing waves is the fundamental mode, whose unique node is on the geomagnetic equatorial plane, with two loops of oscillation on the ends

of the line of force on the earth in both hemispheres. This mode of oscillation has been investigated theoretically by Dungey (1954), who called it the normal mode of torsional oscillations of the magnetic field in the earth's cavity. The eigen-period of these oscillations increases rapidly with the latitude where the magnetic line of force intersects the earth's surface, varying from several tens of seconds to about 10 minutes from the subauroral region to the polar region (Kato and Watanabe, 1956, Obayaski and Jacobs 1958, Obayashi 1958).

In addition to the above mode, there is another mode of oscillation responsible for geomagnetic pulsations of shorter periods. As noted by Dessler (1958), the velocity of Alfvén waves decreases very rapidly with decreasing height in the exospheric region below around 2,000 km. Therefore, due to the continuity of energy flow one can expect Alfvén waves of certain periods coming from the outer exosphere to be intensified. In this mode of oscillation, the layer of maximum Alfvén velocity, which is approximately between 1,500 and 3,000 km, becomes the node of oscillation, and the loop of oscillation is near the earth's surface. This mode of hydromagnetic oscillation corresponds to the geomagnetic pulsations with periods from about one to several seconds, which appear more frequently in night-time than in daytime (Jacobs and Watanabe, 1962).

In considering the above facts, one might speculate that a possible mechanism for the production of infrasonic waves during auroral activity would be the penetration of Alfvén waves, including modified

Alfven waves and retarded sound waves (Obayashi, 1958), through the ionosphere. However, as will be shown later, these contributions are very small as compared with the pressure disturbances produced by the periodic heating of the lower ionosphere caused by auroral bombardments.

As shown by Heppner (1958), auroral activity predominates around midnight local time and the active region extends towards lower latitudes with increasing activity, and pulsating aurorae appear at this phase of auroral activity. In other words, among several types of auroral displays, pulsating aurorae appear with the largest disturbance in energy, and occur in fairly low latitudes.

According to Campbell and Ress (1961), the peak of pulsating aurorae is around 100 km, the height of the bottom is 90 km, the effective thickness is of the order of 20 km, and the most frequent period is from 6 to 10 sec. According to the direct measurement of auroral particles by means of rocket borne detectors, the energy flux of auroral particles, which is mostly electrons, is of the order of several tens of ergs/cm²-sec at weak aurora and it increases by more than a factor of 50 at bright aurora (McIlwain, 1960). Thus, one can estimate that the energy flux in strong pulsating aurora is of the order of 10³ erg/cm²-sec or more. This figure is consistent with the estimate given by Chamberlain (1961) based on measurements of auroral luminosity.

On the other hand, the energy flux of hydromagnetic waves deduced from the magnetic pulsation data is less than 10 erg/cm²-sec below

200 km. The energy flux of hydromagnetic waves increases with height. However, the contribution to pressure waves in the lower atmosphere decreases with increasing height of source, as will be shown later.

Another evidence which favors our present idea is the very good correspondence between the appearance of pulsating aurorae and that of infrasonic waves as shown in Fig. 2. The occurrence of pulsating aurorae shown on the right side of this figure is taken from the Visoplot of auroral activity reported from the IGY Data Center, on days which correspond to the events reported by Chrzanowski et al. (1961), which are shown on the left side of this figure. The arrival direction of these waves might deviate from the true direction due to strong wind systems in high altitudes. Therefore, the appearances of pressure waves do not necessarily match the pulsating auroral events in detail. It is, however, quite clear that there is a close correspondence between the appearance of infrasonic waves and that of pulsating aurorae.

3. Mathematical Treatment.

It is quite obvious that the ray theory is not applicable in this problem, because the wave length is of the order of an atmospheric depth or more for the infrasonic waves observed.

The excitation and propagation of long period pressure waves in the atmosphere have been investigated by several workers, mainly in two fields of geophysics, i.e., meteorology and ionospheric physics. The theoretical aspects of those problems appearing in geophysics, including oceanography, has been recently reviewed by Eckart (1940,

1956, 1960), who has also developed a mathematical technique to solve these problems, introducing the so-called field variables instead of simple hydrodynamical variables.

In the present calculations, however, we shall use rather the classical method based on the equations of velocity divergence, because of its convenience in comparing the results with the observed data.

3.1 Notations and Fundamental Equations.

The notations and constants used are as follows:

| | |
|------------------|---|
| $\vec{g}(0, -g)$ | acceleration of gravity, $g = 980 \text{ cm/sec}^2$; |
| γ | ratio of specific heats of air, i.e., $C_p/C_v \cong 1.4$, where C_p and C_v are the specific heat of air at constant pressure and that at constant volume, respectively; |
| R | gas constant of air, $B/M = 2.87 \times 10^6 \text{ ergs/g-}^\circ\text{C}$, where B is the universal gas constant, $8.314 \times 10^7 \text{ ergs/mol-}^\circ\text{K}$, and M is the molecular weight of air, approximately 28.97; |
| $\vec{\Omega}$ | Coriolis vector, in rad/sec; |
| \vec{f} | resultant of external forces except gravity, dyne/g; |
| η | entropy of air in $\text{erg/g}^\circ\text{K}$; |
| $q'(x, z)$ | rate of net accession of heat, erg/g sec ; and |
| | $s(x, z) = (\gamma-1)q$ where $q = \rho \cdot q'$ in $\text{erg/cm}^3 \text{ sec}$. |

| | |
|--------------------|---|
| x, z | horizontal (southward) and vertical (upward) coordinates; |
| $\vec{U}(u, w)$ | velocity vector, where u is horizontal (southward) and w is upward component of air flow in cm/sec; |
| $\chi(x, z)$ | the divergence of velocity in sec^{-1} , i.e. $\chi = \partial u / \partial x + \partial w / \partial z$; |
| p, ρ, T | small departure from static values of pressure, density, and temperature, function of x and z and t . |
| p_0, ρ_0, T_0 | static pressure, density, and absolute temperature which are the functions of z only in dyne/cm^2 , g/cm^3 and $^{\circ}\text{K}$, respectively, |
| p, ρ, T | total pressure, density and temperature, i.e. $p_0 + p$, $\rho_0 + \rho$ and $T_0 + T$ respectively. |
| p_s, ρ_s, T_s | static value of pressure, of density and of temperature of air at the sea level. |
| l | vertical wave length of pressure wave in cm.. |
| λ | horizontal wave length of pressure wave in cm. |
| τ | period of pressure wave in sec |
| k | horizontal wave number corresponding to λ , in cm^{-1} , i.e. $2\pi/\lambda$. |

σ frequency of pressure wave corresponding to τ , i.e.
 $2\pi/\tau$.

D/Dt the Eulerian derivative, i.e. $\partial/\partial t + \vec{U} \cdot \vec{\nabla}$

c velocity of sound in the atmosphere in cm/sec. $c^2 = \gamma gH$
 where H is the scale height of isothermal atmosphere,
 $H = RT/g$.

In the Eulerian notation, the equation of motion is

$$\frac{D\vec{U}}{Dt} + \frac{1}{\rho} \vec{\nabla} p + \vec{g} + \vec{\Omega} \times \vec{U} = \vec{f} \quad (3.1.1)$$

and the equation of continuity is given by

$$\frac{D}{Dt} \left(\frac{1}{\rho} \right) - \frac{1}{\rho} \vec{\nabla} \cdot \vec{U} = 0. \quad (3.1.2)$$

The variations of pressure due to thermal excitations can be derived from the second law of thermodynamics, which gives the change of entropy (Eckart 1960), i.e.

$$\frac{D\eta}{Dt} = \frac{q'}{T}. \quad (3.1.3)$$

Because of the equation of continuity (3.1.2), it can be shown that Eq. (3.1.3) is equivalent to

$$\frac{Dp}{Dt} - c^2 \frac{D\rho}{Dt} = s(x, z, t). \quad (3.1.4)$$

Since in our present problem the period of oscillation is less than a few minutes, the Coriolis force due to the earth's rotation is negligible,

and all other external forces, except gravity, can be assumed to be zero. The equation of motion for the present problem is then simply written as

$$\frac{D\vec{U}}{Dt} + \frac{1}{\rho_0} \vec{\nabla} p = \vec{g}. \quad (3.1.5)$$

3.2 One Dimensional Model.

For this case the atmospheric motion has only the z -component of velocity, w , therefore, the equation of motion (3.1.5) is written in linear approximation by

$$\rho_0 \frac{\partial w}{\partial t} = - \frac{\partial p}{\partial z} - \rho g. \quad (3.2.1)$$

The equation of continuity in linear approximations is

$$\frac{\partial \rho}{\partial t} + \rho_0 \frac{\partial w}{\partial z} - \frac{\rho_0}{H} w = 0. \quad (3.2.2)$$

The entropy equation (3.1.4) can be written in the present case in linear approximation by

$$\frac{\partial p}{\partial t} = - \rho_0 c^2 \frac{\partial w}{\partial z} + \rho_0 g w + (\gamma - 1) q \quad (3.2.3)$$

where $q = q(z, t)$ is the periodically changing heat source, which can be assumed to be

$$q(z, t) = \begin{cases} q(z) e^{i\sigma t} & \text{for } z \geq 0 \\ 0 & \text{for } -z_0 \leq z < 0 \end{cases} \quad (3.2.4)$$

where

$$q(z) = \frac{q_0 e^{-z/h}}{h} \quad (3.2.5)$$

and q_0 is the maximum rate of heat generation in an atmospheric column with unit cross section in $\text{erg/cm}^2 \text{ sec}$. $z = 0$ is taken as the height of the base of heating, and the earth's surface is given by $z = -z_0$.

Eliminating p and ρ from the above equations, the following differential equation is obtained:

$$\frac{\partial^2 w}{\partial z^2} - \frac{1}{H} \cdot \frac{\partial w}{\partial z} - \frac{1}{c^2} \frac{\partial^2 w}{\partial t^2} = \frac{\gamma - 1}{\rho_0 c^2} \cdot \frac{\partial q}{\partial z}. \quad (3.2.6)$$

For the region $-z_0 \leq z < 0$, where no heat-source exists, w is given by

$$w = \frac{i}{k_2 - k_1} e^{ik_1 z} A + \frac{i}{k_1 - k_2} e^{ik_2 z} B \quad (3.2.7)$$

and for the region $z \geq 0$, where the heat source exists, w is given by

$$w = \frac{i}{k_2 - k_1} e^{ik_1^2 z} \left[\int_0^z e^{-ik_1 \xi} Q(\xi) d\xi + C \right] + \frac{i}{k_1 - k_2} e^{ik_2^2 z} \left[\int_0^z e^{-ik_2 \xi} Q(\xi) d\xi + D \right] \quad (3.2.8)$$

where the constants A, B, C and D are to be determined by the following boundary conditions: (i) at $z \rightarrow \infty$, there should be no wave downward,

(ii) w and p are continuous at the boundary, $z = 0$, and (iii) $w = 0$ at the ground, $z = -z_0$.

The time dependent factor, $e^{i\sigma t}$, is dropped in Eq. (3.2.7), and in Eq. (3.2.8) this will be always dropped hereafter.

Due to the condition (iii), the pressure variation at the ground is given by Eq. (3.2.3) as

$$(p)_{z=-z_0} = \frac{i}{\sigma} \rho_s c^2 \left(\frac{dw}{dz} \right)_{z=-z_0} \quad (3.2.9)$$

where ρ_s is the atmospheric density at the earth's surface.

Substituting Eq. (3.2.7) into Eq. (3.2.9) and by making use of the conditions (i) and (ii), we find

$$\left(\frac{dw}{dz} \right)_{z=-z_0} = e^{-ik_1 z_0} \frac{(\gamma-1)q_0}{\rho_c c^2} \cdot \frac{1}{l} \left(1 - \frac{h}{H} + \frac{h^2}{l^2} \right)^{-1/2} \quad (3.2.10)$$

provided that the angular wave frequency σ is larger than a critical frequency σ_A , defined by

$$\sigma_A = \frac{\gamma g}{2c} \quad (3.2.11)$$

(Maeda and Watanabe, 1963). Thus, the final expression of the amplitude of pressure variations at the ground, caused by the periodic disturbance in the upper atmosphere $q(z, t)$ is

$$p_s = \frac{(\gamma-1)}{c} q_0 \left(\frac{\rho_s}{\rho_c} \right)^{1/2} \left(1 - \frac{h}{H} + \frac{h^2}{l^2} \right)^{-1/2} \quad (3.2.12)$$

The numerical values p_s/q_0 given by Eq. (3.2.12) are plotted in Fig. 3 against h (in km) for several values of angular frequency, σ . The full lines and dashed lines stand for the scale height of 8 km and 6.8 km, respectively. The latter gives proper ratio of $(\rho_e/\rho_s)^{1/2}$ as compared with the observed atmospheric densities.

From this figure, one can see that periodic heating corresponding to a flux of the order of $100 \text{ erg/cm}^2 \text{ sec}$ produces pressure waves with amplitudes of the order of 1 dyne/cm^2 at the ground.

3.3 Two Dimensional Model

3.3.1 Equation of Velocity Divergence

From Eq. (3.1.5), the equation of motion for two dimensional case is

$$\rho_0 \frac{\partial u}{\partial t} = - \frac{\partial p}{\partial x} \quad (3.3.1)$$

$$\rho_0 \frac{\partial w}{\partial t} = - \frac{\partial p}{\partial z} - g\rho. \quad (3.3.2)$$

The equation of continuity, (3.1.2) can be written in first order approximation as

$$\frac{\partial p}{\partial t} + w \frac{\partial \rho_0}{\partial z} = - \rho_0 \chi \quad (3.3.3)$$

where $\chi = \chi(x, z, t)$ is the velocity divergence defined in section (3.1).

Using Eq. (3.3.3), Eq. (3.1.4) can be written as

$$\frac{\partial p}{\partial t} = \rho_0 g w - \rho_0 c^2 \chi + s. \quad (3.3.4)$$

Assuming that the time variations of u , w , p , ρ and s are proportional to a factor $e^{i\sigma t}$, the following relations between u , w and p are obtained from Eqs. (3.3.1), (3.3.2), (3.3.3) and (3.3.4),

$$-\sigma^2 u = \frac{\partial}{\partial x} (c^2 \chi - g w) - \frac{1}{\rho_0} \cdot \frac{\partial s}{\partial x} \quad (3.3.5)$$

$$-\sigma^2 w = c^2 \frac{\partial \chi}{\partial z} - \gamma g \chi + g \frac{\partial u}{\partial x} - \frac{1}{\rho_0} \cdot \frac{\partial s}{\partial x} \quad (3.3.6)$$

and

$$i\sigma p = \rho_0 g w - c^2 \rho_0 \chi + s. \quad (3.3.7)$$

Eliminating u , w and p from above equations, we finally obtain the following differential equation for the velocity divergence, $\chi(x, z)$:

$$\begin{aligned} \nabla^2 \chi + \frac{1}{c^2} \left(\frac{dc^2}{dz} - \gamma g \right) \frac{\partial \chi}{\partial z} - \frac{g}{c^2 \sigma^2} \left(\frac{dc^2}{dz} + (\gamma - 1)g \right) \frac{\partial^2 \chi}{\partial x^2} + \frac{\sigma^2}{c^2} \chi \\ = - \frac{1}{c^2 \sigma^2} \left\{ \frac{g}{\rho_0(z) c^2} \left(\frac{dc^2}{dz} + \gamma g \right) \frac{\partial^2 s}{\partial x^2} - \frac{\sigma^2}{\rho_0 c^2} \left(\frac{dc^2}{dz} + \gamma g \right) \frac{\partial s}{\partial z} - \frac{\sigma^2}{\rho_0} \nabla^2 s \right\} \end{aligned} \quad (3.3.8)$$

(Maeda and Watanabe, 1963).

3.3.2 The Diagnostic Diagram

If there is no thermal excitation, the right hand side of Eq. (3.3.8) is zero, and the solution of this homogenous differential equation

corresponds to the free oscillation of the atmosphere on the non-rotating earth.

We now consider pressure waves traveling horizontally in this flat atmosphere. Assuming that u , w , p , and ρ are proportional to a factor $e^{i(\sigma t - kx)}$, we get an equation for the vertical change of $\chi(\sigma, z)$.

$$\frac{d^2\chi}{dz^2} + \frac{1}{H} (H' - 1) \frac{d\chi}{dz} + \left[\frac{\sigma^2}{\gamma g H} - k^2 + \frac{k^2 g}{\sigma^2 H} \left(H' \frac{\gamma - 1}{\gamma} \right) \right] \chi = 0 \quad (3.3.9)$$

where $H' = dH/dz$, and c^2 is replaced by $\gamma g H(z)$.

For simplicity, let us consider the case of an isothermal atmosphere, where $H' = 0$. Then Eq. (3.3.9) is written as

$$\frac{d^2\chi}{dz^2} - 2N \frac{d\chi}{dz} + M^2 \chi = 0 \quad (3.3.10)$$

where

$$N = 1/2H \quad (3.3.11)$$

and

$$M^2 = \frac{\sigma^2}{c^2} - k^2 + \frac{k^2 g^2}{c^2 \sigma^2} (\gamma - 1). \quad (3.3.12)$$

This differential equation has the following solution:

$$\chi(\sigma, z) = e^{Nz} (Ae^{-\mu z} + Be^{+\mu z}) \quad (3.3.13)$$

where A and B are constant, and

$$\mu^2 = N^2 - M^2 > 0 \text{ for non-cellular solution} \quad (3.3.14)$$

and

$$\mu = i\eta, \quad \eta^2 = M^2 - N^2 > 0 \text{ for cellular solution.} \quad (3.3.15)$$

As was shown by Pekeris (1948), in the non-cellular solution in a single isothermal atmosphere (3.3.13), the term with $e^{\mu z}$ must vanish, (i.e. $B = 0$), otherwise the kinetic energy of non-cellular waves, which is proportional to $\rho_0(z)\chi^2$, diverges. Furthermore, due to another condition that the vertical component of velocity must vanish at the ground, we get only two possible types of free oscillation. The one corresponds to Lamb's wave (Lamb, 1932, p. 548), which exists at all frequencies, while the other can be propagated only above a critical value σ_c , given by

$$\sigma_c = \frac{g}{c} \sqrt{\frac{\gamma}{2}} \quad (3.3.16)$$

(the corresponding period is around 250 sec), and the wave is dispersive.

It should be noted that due to the decrease of atmospheric density, the amplitude of Lamb wave (pressure variation) decreases with altitude by a factor $\exp(-gz/c^2)$, preventing the propagation of waves in any except horizontal directions (Eckart, 1960, p. 106).

On the other hand, for the cellular solution, η stands for the wave number in the vertical direction and equation (3.3.15) is equivalent to

$$\eta^2 c^2 = \frac{(\sigma^2 - \sigma_A^2) + k^2 c^2 (\sigma_B^2 - \sigma^2)}{\sigma^2} \quad (3.3.17)$$

where $\sigma_A = g\gamma/2c$ and $\sigma_B = g(\gamma - 1)^{1/2}/c$. (3.3.18)

Brunt's frequency, σ_B , is the frequency of the vertical oscillation of a free air parcel in the atmosphere, changing adiabatically. This expression was also derived by Väisälä as a stability parameter of the atmosphere (Eckart, 1960). σ_A can be called the critical atmospheric sound frequency, because no acoustic oscillation exists below this frequency in the atmosphere.

The curve $\eta^2 = 0$ consists of two branches, A and B, as shown in Fig. 4, in which σ is plotted against k . The curve A starts from the σ -axis at $\sigma = \sigma_A$, and becomes asymptotic to the line C, which corresponds to the solution of non-cellular Lamb's wave, $\sigma = kc$. The other curve, B, passes through the origin and becomes asymptotic to the horizontal line $\sigma = \sigma_B$.

Following Eckart (1960), Fig. 4 will be called the diagnostic diagram of the isothermal atmosphere, and the waves corresponding to the two domains in which $\eta^2 > 0$ are named as Sonic (mode A) and Thermobaric (mode B), respectively. Sonic and thermobaric waves are also called acoustic and internal gravity waves, respectively, by Hines (1960).

3. Intensity of Pressure Waves at the Ground

Since the source of excitation, $s(x, z)$, is assumed to be limited inside of the auroral zone, the right hand side of Eq. (3.3.8) is not uniform with respect to x . Therefore this differential equation is not in general separable with respect to the variables x and z .

Therefore, the following assumptions are made to solve the equation.

- (i) the atmosphere is isothermal with scale height H .
- (ii) the distribution of heat source is uniform along the y -direction (this is assumed at the beginning to reduce the problem to two dimensions), but it is limited horizontally in the x -direction within $\pm\lambda_0$, i.e. $-\lambda_0 \leq x \leq \lambda_0$, and is extended vertically above a certain height z , i.e. $z \geq z_0$.
- (iii) the time variation of the heat source is periodic with an angular frequency σ , and the same phase within the domain indicated in (ii).

The assumption (i) reduces Γq . (3.3.8) to the following form:

$$\begin{aligned} & \left(1 - \frac{\sigma_B^2}{\sigma^2}\right) \frac{\partial^2 \chi}{\partial x^2} + \frac{\partial^2 \chi}{\partial z^2} - \frac{1}{H} \frac{\partial \chi}{\partial z} + \frac{\sigma^2}{c^2} \chi \\ &= \frac{1}{\rho_0(z) c^2} \left[\left(1 - \frac{g}{\sigma^2 H}\right) \frac{\partial^2 s}{\partial x^2} + \frac{\partial^2 s}{\partial z^2} + \frac{1}{H} \frac{\partial s}{\partial z} \right]. \end{aligned} \quad (3.3.19)$$

The assumptions (ii) and (iii) can be written as

$$s(x, z, t) = s(z) e^{i\sigma t} \theta(z - z_0) [\theta(x + \lambda_0) - \theta(x - \lambda_0)] \quad (3.3.20)$$

where

$$s(z) = \frac{(\gamma - 1) q_0}{h} \exp\left[\frac{-(z - z_0)}{h}\right] \quad (3.3.21)$$

and $\theta(\xi)$ is a unit step-function of ξ , defined by

$$\theta(\xi) = \begin{cases} 1 & \xi \geq 0 \\ 0 & \xi < 0. \end{cases} \quad (3.3.22)$$

It should be noted that q_0 is the maximum rate of heat-release in an atmosphere in an air column of unit cross-section, ergs/sec cm².

Since the atmosphere is assumed to be isothermal, the density of air in equilibrium at height z is given by

$$\rho_0(z) = \rho_s e^{-\frac{z}{H}}. \quad (3.3.23)$$

In order to solve Eq. (3.3.19) under the conditions listed above, the following Fourier transforms are applied with respect to x ,

$$X(k, z) = \frac{1}{\sqrt{2\pi}} \int_{-\infty}^{\infty} e^{ikx} \chi(x, z) dx \quad (3.3.24)$$

and

$$S(k, z) = \frac{1}{\sqrt{2\pi}} \int_{-\infty}^{\infty} e^{ikx} s(x, z) dx. \quad (3.3.25)$$

Since the heat source $s(x, z)$ vanishes outside of the auroral zone, both $s(x, z)$ and $\chi(x, z)$ must vanish at $x = \pm\infty$. Thus we get

$$\frac{1}{\sqrt{2\pi}} \int_{-\infty}^{\infty} \frac{\partial^2 \chi}{\partial x^2} e^{ikx} dx = -k^2 X(k, z) \quad (3.3.26)$$

and

$$\frac{1}{\sqrt{2\pi}} \int_{-\infty}^{\infty} \frac{\partial^2 S}{\partial x^2} e^{ikx} dx = -k^2 S(k, z). \quad (3.3.27)$$

Using these transforms, Eq. (3.3.19) is written as

$$\frac{d^2 X}{dz^2} - 2N \frac{dX}{dz} + M^2 X = F(k, z) \quad (3.3.28)$$

where

$$F(k, z) = \frac{1}{c^2 \rho_0(z)} \left[\frac{d^2 S}{dz^2} + \frac{1}{H} \frac{dS}{dz} - k^2 \left(1 - \frac{g}{\sigma H} \right) S \right] \quad (3.3.29)$$

and N, M^2 are the same as in Eq. (3.3.11) and Eq. (3.3.12). The total solution of Eq. (3.3.28) can be written as

$$X(k, z) = e^{n_1 z} \left[C_1 + \frac{1}{2\mu} \int_0^z F(z') e^{-n_1 z'} dz' \right] + e^{n_2 z} \left[C_2 + \frac{1}{2\mu} \int_0^z F(z') e^{-n_2 z'} dz' \right] \quad (3.3.30)$$

where n_1 and n_2 are the roots of the following characteristic equation

$$n^2 - 2Nn + M^2 = 0 \quad (3.3.31)$$

$$\text{and we assume; } n_1 = N - \mu \text{ and } n_2 = N + \mu \quad (3.3.32)$$

where μ is given by Eq. (3.3.14) or by Eq. (3.3.15) for non-cellular or cellular solution, respectively.

The integration constants C_1 and C_2 are determined by the following two boundary conditions:

(i) the vertical component of the velocity vanishes at the ground, i.e.,
 $w(x, z = 0) = 0$ (3.3.33)

(ii) the kinetic energy of the waves at $z = \infty$ is either zero or remains finite. In the latter case, the vertical component of the disturbance should be propagated upwards only at $z = \infty$.

The pressure change at the ground can be obtained by $\chi(x, z = 0)$, which is given by the inverse Fourier transform of $X(k, z = 0)$, i.e.

$$\chi(x, 0) = \frac{1}{\sqrt{2\pi}} \int_{-\infty}^{\infty} e^{-ixk} X(k, 0) dk \quad (3.3.34)$$

where $\chi(k, 0)$ is the solution of Eq. (3.3.28) at $z = 0$ satisfying the above conditions, and is given by

$$X(k, 0) = \sqrt{\frac{2}{\pi}} \cdot \frac{(\gamma-1) q_0}{h \sigma^4 c^2 \rho_0} e^{\frac{z_0}{2H} - \mu z_0} \cdot \frac{\sin \lambda_0 k}{k} \cdot \frac{\sigma^4 - k^2 g^2}{(n_1 - m)(n_2 + \beta)} \quad (3.3.35)$$

where

$$m(\sigma) = g \left(\frac{\gamma}{c^2} - \frac{k^2}{\sigma^2} \right) \quad (3.3.36)$$

and

$$\beta = \frac{1}{h} - \frac{1}{H}. \quad (3.3.37)$$

Since $w(x, 0) = 0$, $s(x, 0) = 0$, and Eq. (3.3.7) can be reduced to

$$p(x, 0) = - \frac{c^2 \rho_s}{i\sigma} \cdot \chi(x, 0) \quad (3.3.38)$$

where $\chi(x, 0)$ is given by the inverse Fourier transform of Eq. (3.3.35).

The evaluations of $p(x, 0)$ are given in the Appendix and the results are shown in Tables I and II, and in Figs. 5 and 6, where p_c and p_{nc} stand for cellular and non-cellular waves, respectively.

4. Discussion

4.1 Attenuation

Due to the viscosity and thermal conductivity of air, acoustic waves in the atmosphere attenuate. The attenuation coefficient, $\alpha(\tau)$ in cm^{-1} for a wave of period τ is given approximately by (Rayleigh, 1929)

$$\alpha(\tau) = \frac{4\pi^2}{\tau^2} \cdot \frac{1}{c^3} \left[\frac{4}{3} \nu + \frac{\gamma - 1}{\gamma} a^2 \right] \quad (4.4.1)$$

where the coefficient of kinematic viscosity ν is given approximately by

$$\nu = \frac{1.7 \times 10^{-4}}{\rho(z)} \text{ in cm}^2/\text{sec} \quad (4.1.2)$$

and the coefficient of thermal conductivity a^2 is given by

$$a^2 = \frac{2.1 \times 10^{-5}}{\rho(z)} \text{ in cm}^2/\text{sec.} \quad (4.1.3)$$

Since the air density ρ decreases with height exponentially, a^2 and ν increase with altitude exponentially. The so-called attenuation factor,

$$f_a(\tau, z) = \exp \left[- \int_0^z a(\tau, z') dz' \right] \quad (4.1.6)$$

is shown in Fig. 7 as a function of the height z in km, for $\tau = 10$ sec, 30 sec and 100 sec.

It should be noticed that the relative amplitude of the pressure wave grows as it propagates upward with a factor $e^{z/2H}$, where H is the scale height, while the absolute amplitude decreases with height by a factor $e^{-z/2H}$, because of the exponential decrease of air density (Schrödinger, 1917). Provided that the amount of excitation energy is the same, therefore, the absolute intensity of the pressure wave at the ground is larger when the base of the excitation level is higher. This is shown by Eqs. (3.2.12) and (3.3.35) with a factor $e^{z_0/2H}$ for $p_s, p_c (z = 0)$ and $p_{nc} (z = 0)$, and by a curved dash line in Fig. 7.

However, due to the steep increase of kinematic viscosity of air with altitude, the yield of pressure wave excitation drops sharply above a certain altitude for a given period (or frequency) of the wave. This is shown in Fig. 8 for three different wave periods $\tau = 10, 30$ and 100 sec. One can see from this figure that there is an effective height of excitation of atmospheric acoustic wave for a given period and this height increases with period.

4.2 Conditions for Wave Formation

According to the calculations in section 3, the pressure variation at the ground of the order of 1 dyne/cm^2 can be expected if the maximum rate of heat generation is of the order of $100 \text{ erg/cm}^2 \text{ sec}$ and if the layer of periodic heating is around 100 km altitude with thickness less than 10 km . Electrons with energy of the order of 100 kev will lose their energy mostly within a layer of the order of 10 km thickness around the height of 100 km (Chamberlain 1961, p. 290). According to Chamberlain, the rate of heat-generation is the order of $60 \text{ erg/cm}^2 \text{ sec}$ in a bright aurora. Therefore, if the rate of heat-generation changes with this order of amplitude periodically, barometric oscillations of the order of 1 dyne/cm^2 at sea level can be expected from those sources in the upper atmosphere.

However, several other conditions must be satisfied, in order that the energy brought into the upper air by auroral electrons can be converted efficiently to pressure waves in the atmosphere.

At first, the time τ_1 in which an electron arriving at auroral height from outer space should be smaller than the period, τ , of the waves concerned. If $\tau \gg \tau_1$, the phase of the time variation of the source differs from place to place, and the resultant pressure wave originating from those different sources would be weakened by superposition.

Since the auroral electrons, whose velocity is of the order of 10^9 cm/sec , lose their energy within a layer of 10 km thickness, $\tau_1 \lesssim 10^{-4}$

sec. This is much smaller than the period of the acoustic waves we consider here.

As discussed by Hansen and Johnson (1960), electrons impinging into the upper atmosphere lose their energy mostly by inelastic collisions with neutral air particles until ≈ 2 ev, which is the lowest excitation energy of atomic oxygen (1D -state). The time, τ_2 , for 1D excitation collisions with oxygen atoms is of the order of 10^{-3} sec at 100 km and of the order of 1 sec at 400 km.

Below 2 ev, the electrons lose energy in the upper atmosphere mainly by elastic collisions with ambient electrons. The time for those low energy electrons to equilibrate with ambient electrons, τ_3 , is obtained from the expression for the rate of energy loss of a fast electron immersed in a thermalized plasma (Hansen & Johnson 1960), and is

$$\tau_3 \approx \frac{5.7 \times 10^3 E^{3/2}}{N_e} \quad (4.2.1)$$

where E is the electron energy, i.e., $E \approx 2$ ev, and N_e is the electron concentration in cm^{-3} .

The equilibration time, τ_3 , given by this expression is about 0.1 sec at 100 km and of the order of 10^{-2} sec above 350 km. Thus $\tau_2 + \tau_3$ is still much smaller than the periods of acoustic waves under discussion.

It should be noted, however, that elastic collisions with neutral particles dominate over those with ambient electrons below the F2 maximum (around 300 km). The time constant, τ_4 for these elastic collisions

consists of $\tau(O)$ and $\tau(N_2)$, the time constants for the loss of excess electron energy to atomic oxygen and to molecular nitrogen, respectively, and is given by

$$\tau_4 = \frac{2.08 \times 10^{11} E^{-1/2}}{n(O) + 2.36n(N_2)} \quad (4.2.2)$$

where $n(O)$ and $n(N_2)$ are the concentration of atomic oxygen and molecular nitrogen per cm^3 , respectively.

For $E = 2$ ev, τ_4 is of the order of 0.1 sec at 100 km and increases with height. For example, it is of the order of 100 sec at 350 km.

As shown in the previous section, the excitation of atmospheric pressure waves above 200 km is not important; the time constant τ_4 , does not destroy the condition of wave formation. In other words, below 200 km $\tau_1 + \tau_2 + \tau_3 + \tau_4 \lesssim \tau$ is satisfied.

Another condition necessary to wave formation is that the time constant for cooling in a certain domain of auroral activity must be much longer than the period of oscillation.

If the initial temperature T_0 is assumed to be horizontally uniform within the domain of the source, $-\lambda_0 \leq x \leq \lambda_0$, then the temperature at the center after $t(\text{sec})$ is approximately,

$$T(t) = (T_0 - T_a) \Phi\left(\frac{\lambda_0}{2\sqrt{a^2 t}}\right) \quad (4.2.3)$$

where

$$\Phi(y) = \frac{2}{\sqrt{\pi}} \int_0^y e^{-x^2} dx \quad (4.2.4)$$

a^2 is the thermal diffusivity (coefficient of thermal conduction) of air, and T_a is the temperature outside of the source.

The time, t_a , necessary to reduce the initial temperature difference between the inside and outside of the source region can be estimated by

$$\Phi\left(\frac{\lambda_0}{2\sqrt{a^2 t_a}}\right) = \frac{1}{2} \quad \text{or} \quad t_a \approx \frac{\lambda_0^2}{a^2}. \quad (4.2.5)$$

Since the thermal diffusivity of air a^2 at a height $z_0 = 100$ km is of the order of 10^6 cm²/sec (see Eq. 4.1.3), the minimum source width needed to satisfy the condition for thermal oscillation is of the order of 30 m for a period of 10 sec, and of the order of 100 m for a period of 100 sec.

The source width considered in our present calculation is significantly larger than these widths. In other words, the time constant for source cooling is sufficiently long for pressure wave production.

4.3 Other Possible Mechanisms

4.3.1 Periodic Heating Due to Absorption of Hydromagnetic Waves.

As stated in the introduction, hydromagnetic waves from the magnetosphere lose part of their energy in the lower exosphere and in the ionosphere. The remaining energy leaking through the ionosphere is

observed as fluctuations of the geomagnetic field intensity, or geomagnetic pulsations.

The rate of energy dissipation of hydromagnetic waves in the ionosphere increases with increasing frequency (Watanabe, 1957; Francis and Karplus, 1960; Akasofu, 1960). According to Watanabe (1957), the dissipation of the hydromagnetic wave energy in the ionosphere is negligible for waves with periods longer than 20 sec. In the auroral region, the amplitude of geomagnetic pulsations sometimes exceed several tens of gamma (i.e., giant pulsations) with periods longer than several tens of seconds. The intensity of the incident wave is usually smaller for higher frequencies (Jacobs and Watanabe, 1962). As shown by the power density of the small scale fluctuations of magnetic field intensity observed in the earth's magnetosphere between 5 and 15 earth's radii (Sonnet et al. 1960), the frequency spectrum of hydromagnetic waves, which are regarded as the origins of geomagnetic pulsations observed at the earth's surface, is a decreasing function of frequencies above the ionosphere. In any case, the upper limit of the incident wave amplitude may be taken as 100γ . The energy flux associated with these hydromagnetic waves is then of the order of several $\text{ergs cm}^{-2}\text{-sec}^{-1}$, assuming that the Alfvén wave velocity above the ionosphere is of the order of 10^8 cm/sec.

The rate of heat generation by absorption of these hydromagnetic waves in the upper ionosphere has been estimated by several authors. (Dessler, 1959; Akasofu, 1960; Francis and Karplus 1960) and their

results are shown in Table III. The rate of heat generation is generally smaller than $1 \text{ erg/cm}^2 \text{ sec}$, except where the period is 1 sec. Therefore the amount of heat generated by hydromagnetic waves penetrating the ionosphere is smaller than that due to the auroral particles. Table III contains also estimations of the thickness of the layer of heat generation. In every case, the thickness is much larger for hydromagnetic waves than for auroral particles.

As shown in Figure 8, the effective height of pressure wave generation by periodic heating of the upper air is limited, and is lower for the shorter period. Therefore, generation of acoustic waves by the attenuation of hydromagnetic waves is less efficient than by the periodic heating due to auroral particles, even if the energy flux of the incident wave is increased to the same amount of the latter.

4.3.2 Pressure Waves Due to the Impacts of Auroral Particles.

A particle coming down into the atmosphere loses its energy by transferring its downward momentum to the air particles. A pressure wave can be generated if the flux of particle changes periodically in time. The upper limit of the pressure intensity by this process can be estimated by assuming that all the incoming particles would stop in a very short time within a very thin layer.

Assuming the average energy of incident electrons is 6 kev and the maximum flux is of the order of $10^{10} \text{ cm}^{-2} \text{ sec}^{-1}$, the maximum pressure thus exerted upon the thin layer of virtual shock absorber is estimated to be of the order of $4 \cdot 10^{-8} \text{ dynes/cm}^2$. The corresponding

intensity at the earth's surface is of the order of 10^{-5} dyne/cm², if all electrons stop at an altitude of 100 km.

4.3.3 Penetration of Hydromagnetic Waves Through the Ionosphere.

As mentioned above, most geomagnetic pulsations are due to hydromagnetic oscillations in the exosphere. These oscillations are related to electromagnetic oscillations in the space between the earth's surface and the lower boundary of the ionosphere. Any oscillation mode in which the compression of atmospheric matter is involved gives rise to a variation in the density, and consequently a pressure variation. Therefore, it may be possible that geomagnetic pulsations and microbarometric oscillations come from the same origin, i.e., hydromagnetic oscillations of the earth's exosphere.

The origins of this kind of pulsation presumably exist in the outer boundary of earth's magnetosphere near the geomagnetic equatorial plane, and it may be propagated as a modified Alfvén wave. A modified Alfvén wave is a transverse wave with respect to changes in the electric and magnetic fields. On the other hand, it is a longitudinal wave when viewed as fluid motion (Van de Hulst 1949). In the space between the earth's surface and the lower boundary of the ionosphere, we should have an electromagnetic wave as well as a pressure wave. The energy flux associated with an incident modified Alfvén wave is roughly $(B^2/8\pi)V_A$, where V_A is the group velocity of the modified Alfvén waves and can be taken as the Alfvén wave velocity at a higher portion of

ionosphere. B is the amplitude of the wave, i.e., the intensity of magnetic fluctuation above the ionosphere.

Assuming conservation of energy flux, the upper limit of the amplitude of the pressure wave at the earth's surface, p_e , can be estimated roughly by,

$$\frac{1}{2} \frac{p_e^2}{c_s \rho_s} = \frac{B^2}{8\pi} V_A$$

where c_s is the sound wave velocity at the earth's surface, and ρ_s is the air density at the earth's surface.

Taking $V_A = 3 \cdot 10^7$ cm/sec, corresponding to the daytime at the sunspot maximum activity, and $B = 30\gamma$, $c_s = 3 \cdot 10^4$ cm/sec, $\rho_s = 1.25 \cdot 10^{-3}$ g/cm³, one gets $p_s \approx 3$ dynes/cm².

In this estimation, the conversion factor between energies of incident Alfvén waves and that of secondary pressure waves is assumed to be unity. However, this factor must be very small due to reflections and energy dissipations of incident waves at the upper part of the ionosphere. If this factor is not small, one could see the appearance of infrasonic waves in the equatorial region during strong magnetic disturbances. Since the occurrence of aurorae in these regions is negligible, this might give a direct detection of modified Alfvén waves coming into the earth's atmosphere from the magnetosphere.

5. Summary

We have shown that one of the most plausible mechanisms for pressure wave generation during geomagnetic disturbances is the periodic heating of the polar ionosphere by auroral particles, observed as pulsating aurorae. As emphasized by Campbell (1962), the main energy source for this type of auroral activity is not only incident auroral particles, but also a flow of secondary electrons called the electro-jet. In this case, periodic heating by these intermittent electric currents is essentially the same as the so-called Joule heating discussed by Cole (1962).

As the results of the present calculation, the following conclusions can be drawn:

- (i) From Figs. 3, 5, and 6, one can see that an incident energy flux of more than $100 \text{ ergs/cm}^2\text{-sec}$ will produce acoustic waves observable at the ground, provided the periods are longer than about 10 seconds.
- (ii) The relative intensity of the pressure wave at the ground is higher when the heating is concentrated within a thin layer than when it is distributed over a wide range of altitudes (Fig. 3 and 5).
- (iii) The intensity ratio between the inside of the source region and the outside is smaller for longer periods, as expected.
- (iv) Similarly, the gradient of intensity around the boundary of the source is steeper when the width of the source is wider.

- (v) The ratio of non-cellular wave intensity to cellular is of the order of 10^{-5} for $\tau = 10$ sec and 10^{-3} for $\tau = 100$ sec, inside of the source. Although the non-cellular intensity exceeds the cellular one at large distances from the source, the contribution of the non-cellular wave to the observed intensity would be negligible, because both waves attenuate in long distance propagation.
- (vi) According to the present calculations, which are based on an isothermal atmosphere, the intensity of acoustic waves more than several hundred km from the region of auroral activity is negligible. Considering the real atmosphere one can conclude, therefore, that the horizontal propagation of acoustic waves through the ducts around the mesopause and the stratopause is rather important to explain the diurnal variation of arrival direction of these waves during the period of high geomagnetic activity shown in Fig. 1.
- (vii) It should be noted, however, that auroral activities are not within the auroral zone but rather extended toward lower latitudes (nearly to 50°N), when these sonic waves are observed during the periods of magnetic disturbances, as can be seen from the auroral visoplots shown in Fig. 2.

To show the position and structure of sonic ducts as well as attenuation of the waves, one must take into account the actual atmospheric temperature distributions. This will be, however, discussed elsewhere (Maeda, 1963).

Finally, it should be noted that the energy flux of acoustic waves at the ground S in $\text{erg/cm}^2 \text{ sec}$ is,

$$S = E \cdot c \quad (5.1)$$

where

$$E = \frac{p_s^2}{2\rho_s c^2} \quad (5.2)$$

and p_s and ρ_s are the maximum amplitude of pressure change in dyne/cm^2 and the static density of air at sea level, respectively, and c is the sound velocity in cm/sec .

Since ρ_s is of the order of $1.25 \times 10^{-3} \text{ g/cm}^3$, the energy flux corresponding to $p_s = 1 \text{ dyne/cm}^2$ is approximately $1.4 \times 10^{-2} \text{ erg/cm}^2 \text{ sec}$. To see the energy relation between the input power and the observed output intensity, as shown in Figs. 3, 5, and 6, the above relation must be used.

ACKNOWLEDGMENTS

The authors wish to express their appreciation to Dr. J. M. Young and his co-workers in the National Bureau of Standards in Washington, D. C., who gave us detailed information on their observations of infrasonic waves during magnetic disturbances. Their thanks are also due to Dr. G. D. Mead for his helpful comments, and Mr. E. Monasterski for his kind help on the computer calculations.

Table I

Intensity of cellular mode of infrasonics on the ground below the center of the source in units of q_0 for three different periods of the waves,

$|p_c|/q_0$

| | $h = H$ | $h = 1/2H$ |
|------------------------------|-----------------------|-----------------------|
| $\lambda_0 = 1 \text{ km}$ | | |
| $\tau = 10 \text{ sec}$ | 6.75×10^{-6} | 1.34×10^{-5} |
| 30 sec | 6.28×10^{-5} | 1.23×10^{-4} |
| 100 sec | 6.92×10^{-4} | 1.06×10^{-3} |
| $\lambda_0 = 10 \text{ km}$ | | |
| $\tau = 10 \text{ sec.}$ | 1.83×10^{-5} | 3.65×10^{-5} |
| 30 sec. | 4.38×10^{-4} | 8.58×10^{-4} |
| 100 sec. | 6.67×10^{-3} | 1.02×10^{-2} |
| $\lambda_0 = 100 \text{ km}$ | | |
| $\tau = 10 \text{ sec.}$ | 1.83×10^{-5} | 3.65×10^{-5} |
| 30 sec. | 4.94×10^{-4} | 9.67×10^{-4} |
| 100 sec. | 1.83×10^{-2} | 2.83×10^{-2} |

Table II

Maximum intensity of non-cellular waves on the ground p_{nc} in units of q_0 , and its ratio to that of cellular waves, $p_{nc}/|p_c|$, for three different periods of the waves. x_0 is the horizontal distance in km of the first nodal lines from the center of the source, of which horizontal width is assumed to be $\lambda_0 = 10$ km.

| | p_{nc} | $p_{nc}/ p_c $ | x_0 |
|------------------|-----------------------|-----------------------|---------|
| <hr/> | | | |
| $h = H$ | | | |
| $\tau = 10$ sec. | 1.28×10^{-9} | 7.0×10^{-5} | 0.85 km |
| 30 sec. | 3.24×10^{-8} | 7.4×10^{-5} | 2.56 km |
| 100 sec. | 1.10×10^{-5} | 1.66×10^{-3} | 8.30 km |
| <hr/> | | | |
| $h = 1/2H$ | | | |
| $\tau = 10$ sec. | 1.11×10^{-9} | 3.03×10^{-5} | 0.85 km |
| 30 sec. | 2.73×10^{-8} | 3.18×10^{-5} | 2.56 km |
| 100 sec. | 1.02×10^{-5} | 9.8×10^{-4} | 8.30 km |
| <hr/> | | | |

Table III

Rate of heat-generation due to attenuation of hydromagnetic waves.

| | Period of HM-waves (second) | rate of heat generation in air-column (erg/sec/cm ²) | thickness of heating layer (km) | altitude of the center of heat- generating layer (km) |
|-------------------------------|--------------------------------------|---|---------------------------------------|--|
| Dessler (1959) | 1 | 1.3 | 200 | 170 |
| Francis- Karplus (1960) | 6.3 | 0.7 | 50 | 125 |
| Akasofu (1960) | 1 | 9.7 | >>200 | 225 |
| | 10 | 0.17 | >200 | 225 |
| | 100 | 0.028 | ≥200 | 225 |

REFERENCES

- Akasofu, S., "On the ionospheric heating by hydromagnetic waves connected with geomagnetic micropulsations," J. Atm. Terr. Phys. 18, 160-173, 1960.
- Campbell, W.H., "Natural Electromagnetic Energy Below the ELF Range," Jour. of Research of N.B.S. 64D, No. 4, 409-411, 1960.
- Campbell, W.H., and Rees, M.H., "A Study of Auroral Coruscations," J. Geophys. Res. 66, 41-55, 1961.
- Campbell, W.H., "Theory of Geomagnetic Micropulsations," AGU-Annual meeting at Washington, D.C., April 28, 1962.
- Chamberlain, J.W., "Physics of the Aurora and Airglow," Academic Press, N. Y., 1961.
- Cole, D.K., "A Source of Energy for the Ionosphere," Nature 194, 75, 1962, "Atmospheric Blow-up at the Auroral Zone," Nature 194, 761, 1962.
- Chrzanowski, P., Greene, G., Lemon, K.T., and Young, J.M., "Traveling pressure waves associated with geomagnetic activity," Jour. Geophys. Res. 66, 3727-3733, 1961.

- Dessler, A.J., "The Propagation Velocity of World-Wide Sudden Commencements of Magnetic Storms," J. Geophys. Res. 63, 405-411, 1958.
- Dessler, A.J., "Ionospheric Heating by Hydromagnetic Waves," J. Geophys. Res. 64, 397-401, 1959.
- Dungey, J.W., "The Propagation of Alfvén Waves through the Ionosphere," Pennsylvania State Univ. Sc., Rep. No. 57, 1954.
- Eckart, C., The Thermodynamics of Irreversible Processes I. The Simple Fluid, Phys. Rev. 58, 267-269, 1940.
- Eckart, C., The Thermodynamics of Irreversible Processes II. Fluid Mixtures, Phys. Rev. 58, 269-275, 1940.
- Eckart, C., and Ferris, H.G., Equation of Motion of the Ocean and Atmosphere, Rev. Mod. Phys. 28, 48-52, 1956.
- Eckart, H.C., Hydrodynamics of Oceans and Atmospheres, Pergamon Press, New York, 1960.
- Francis, W.E., and Karplus, R., "Hydromagnetic Waves in the Ionosphere," J. Geophys. Res. 65, 3593-3600, 1960.
- Fukushima, N., Comments at the seminar at Univ. of Md., Nov. 8, 1960.
- Hanson, W.B., and Johnson, F.S., "Electron Temperature in Ionosphere," Memo. Roy. Soc. Sci. Liege, 4, 390-423, 1960.

- Heppner, J.P., A Study of Relationships between the Aurora Borealis and the Geomagnetic Disturbances caused by Electric Currents in the Ionosphere," DRB Canada, Report No. DR-135, 1958.
- Heppner, J.P., Ness, N.F., Skillman, T.L., and Searrce, C.S., Contribution to 1961 Kyoto Conference 1-13, "Magnetic Field Measurements with Explorer X Satellite, 1961," "Explorer 10 Magnetic Field Measurements," J. Geophys. Res. 68, 1-46, 1963.
- Hines, C.O., Internal Atmospheric Gravity Waves at Ionospheric Heights, Canad. J. Phys. 38, 1441-1481, 1960.
- Jacob, J.A., and Watanabe, T., "Propagation of Hydromagnetic Waves in the Lower Exosphere and the Origin of Short Period Geomagnetic Pulsations," J. Atm. Terr. Phys. 24, 413-434, 1962.
- Kato, Y., and Watanabe, T., "Further Study on the Cause of Giant Pulsations," Sci. Rep. Tohoku Univ. Ser. 5, Geophysics 8, 1-10, 1956.
- Lamb, H., Hydrodynamics, Dover Pub., N.Y., 1932
- Maeda, K., "On the Acoustic Heating of the Polar Night Mesosphere," NASA Tech. Note, Jour. Geophys. Res. (in press)
- Maeda, K., and Watanabe, T., "Pulsating Aurorae and Infra-Sonic Waves in the Polar Atmosphere," NASA Tech. Note, 1963.

- Martyn, D.F., Cellular Atmospheric Waves in the Ionosphere and Troposphere, Proc. Roy. Soc. A201, 216-233, 1950.
- McIlwain, C.E., Direct Measurement of Particles Producing Visible Aurorae, Ph.D. Thesis, State Univ. of Iowa, 1960, J. Geophys. Res. 65, 2727-2747, 1960.
- Obayashi, T., and Jacobs, J. A., "Geomagnetic Pulsations and the Earth's Outer Atmosphere" Geophys. J. Roy. Astro. Soc., 1, 53-63, 1958.
- Obayashi, T., Geomagnetic Storms and the Earth's Outer Atmosphere. Report of Ionos. Res. in Japan 12, 301-335, 1:958.
- Pekeris, C.L., The Propagation of a Pulse in the Atmosphere. Part II, Phys. Rev. 73, 145-154, 1948.
- Rayleigh, J.W.S., The Theory of Sound, Vol. II, Cambridge Trans. p. 315, 1929.
- Schrödinger, E., "Zur Akustik der Atmosphäre," Phys. Zeits, 18, 445-453, 1917.
- Sholte, J.G. and Veldkamp, J., Geomagnetic and Geoelectric Variations, J. Atm. Terr. Phys. 6, 33-45, 1955.
- Sonnet, C.P., Judge, D.L., Sims, A.R., and Kelso, J.M., A Radical Rocket Survey of the Distant Geomagnetic Field, J. Geophys. Res. 65, 55-68, 1960.

Van de Hulst, H.C., "Interstellar Polarization and Magneto-Hydrodynamic Waves," Proc, Sympo. on Cosm. Aerodyn. Paris, 1949.

Watanabe, T., "Electrodynamical Behaviour and Screening Effect of the Ionosphere," Sci. Rep. Tohoku Univ. Ser. 5, 9, 81-98, 1957.

Watanabe, T., "Law of electric conduction for waves in the ionosphere," J. Atm. Terr. Phys. 24, 117-125, 1962.

APPENDIX

Evaluations of $p(x, 0)$

As it can be seen from Eq. (3.3.35), $\chi(k, 0)$ is an even function of k . Therefore, the substitution of Eq. (3.3.35) into Eq. (3.3.34) gives:

$$\chi(x, 0) = \frac{2}{\pi} \cdot \frac{(\gamma - 1) q_0 \sigma^2}{h k_g^2 \rho_s c^4} e^{\frac{z_0}{2H}} \int_0^\infty e^{-\mu z_0} \frac{\cos k \sin \lambda_0 k}{k} \cdot \frac{k_g^2 - k^2}{(n_1 - m)(n_2 + \beta)} dk \quad (A.1)$$

where

$$k_g = \frac{\sigma^2}{g}. \quad (A.2)$$

Since μ is a real function of k for $k \geq k_c$ and complex for $0 \leq k \leq k_c$,

where

$$k_c = \frac{\sigma}{c} \sqrt{\frac{\sigma^2 - \sigma_A^2}{\sigma^2 - \sigma_B^2}}. \quad (A.3)$$

Eq. (A.1) can be written further

$$\chi(x, 0) = \chi_c(x, 0) + \chi_{nc}(x, 0) \quad (A.4)$$

where

$$\chi_c(x, 0) = \frac{2}{\pi} \cdot \frac{(\gamma - 1) q_0 \sigma^2}{h k_g^2 \rho_s c^4} e^{\frac{z_0}{2H}} \int_0^{k_c} e^{-i\eta z_0} \frac{\cos xk \sin \lambda_0 k}{k} \cdot \frac{k_g^2 - k^2}{(n_1 - m)(n_2 + \beta)} dk \quad (A.5)$$

and

$$\chi_{nc}(x, 0) = \frac{2}{\pi} \frac{(\gamma - 1) q_0 \sigma^2}{h k_g^2 \rho_s c^4} e^{\frac{z_0}{2H}} \int_{k_c}^{\infty} e^{-\mu z_0} \frac{\cos xk \sin \lambda_0 k}{k} \frac{k_g^2 - k^2}{(n_1 - m)(n_2 + \beta)} dk \quad (A.6)$$

The integrand of $\chi_{nc}(x, 0)$ has two singular points $k_1 = \sigma/c$ and $k_g = \sigma^2/g$, corresponding to the two types of free oscillations of non-cellular mode which are pointed out by Pekeris (1948). Because of a steep exponential term $e^{-\mu z_0}$, however, contributions of these singularities to the integral is not so important as the contribution from the narrow band near $k \gtrsim k_c$, where the exponential term is nearly unity.

The integrand of χ_c has no singularities but oscillates by the term $e^{-i\eta z_0}$. The main contribution arises also from a narrow domain near $k \lesssim k_c$. Substituting Eq. (A.4) into Eq. (3.3.38), we get

$$p(x, 0) = p_c(x, 0) + p_{nc}(x, 0) \quad (A.6)$$

where $p_c(x, 0)$ and p_{nc} correspond to $\chi_c(x, 0)$ and $\chi_{nc}(x, 0)$ respectively.

FIGURE CAPTIONS

Fig. 1 - Diurnal variation of arrival direction of infrasonic waves during magnetic storms observed at the National Bureau of Standards, Washington, D.C. (Reproduced from the data reported by Chrzanowski et al., 1961). The three figures on the right hand side indicate the shifts of the source of these pressure waves, corresponding to the movement of auroral activity.

Fig. 2 - Diurnal variation of the arrival of infrasonic waves during specific magnetic storms detected at the National Bureau of Standards, Washington, D.C. (Chrzanowski et al.), and corresponding auroral activities observed in the northern hemisphere.

Fig. 3 - Relative intensity of pressure waves on the ground produced by periodic auroral heating, vs the scale height of the heat source, in the one dimensional model with an isothermal atmosphere. Full lines and dashed lines correspond to scale heights for an isothermal atmosphere of $H = 8$ km and $H = 6.8$ km, respectively. The parameter attached to each line is the angular frequency, $\sigma = 2\pi/\tau$, where τ is the period of the wave in sec.

Fig. 4 - Diagnostic diagram for an isothermal atmosphere with scale height $H = 8$ km. ($T_0 = 273$ K). See text for meaning of symbols.

Fig. 5(a) - Intensity of cellular waves produced by periodic auroral heating, $|p_c|$ in units of q_0 , vs the horizontal distance from the center of the source for wave period $\tau = 10$ sec. Full lines and dashed lines stand for $h = H$ and $h = 1/2H$, respectively.

Fig. 5(b) - Intensity of cellular waves produced by periodic auroral heating, $|p_c|$ in units of q_0 , vs the horizontal distance from the center of the source for wave period $\tau = 30$ sec. Full lines and dashed lines stand for $h = H$ and $h = 1/2H$, respectively.

Fig. 5(c) - Intensity of cellular waves produced by periodic auroral heating, $|p_c|$ in units of q_0 , vs the horizontal distance from the center of the source for wave period $\tau = 100$ sec. Full lines and dashed lines stand for $h = H$ and $h = 1/2H$, respectively.

Fig. 6 - Intensities of cellular waves on the ground in the units of q_0 vs horizontal distance x in km from the center of the source, of which width λ_0 is 100 km, for $\tau = 10$ sec, 30 sec and 100 sec, respectively.

Fig. 7 - Attenuation factor $f_a(\tau, z)$ vs altitude of the source z_0 in km. Dashed lines indicate

$$-\ln f_a(\tau, z) = \int_p^z a(\tau, z') dz' \quad (\text{straight lines})$$

for $\tau = 10, 30$, and 100 sec and the exponential amplification factor, $\ln(\rho_z/\rho_0)^{1/2} \simeq z/2H$, where the scale height, H , is assumed to be 8 km.

Fig. 8 - Relative yield of the source to the infrasonic waves in the isothermal atmosphere

$$\sqrt{\frac{\rho(z)}{\rho_0}} f_a(\tau, z) \simeq \exp \left[\frac{z}{2H} - \int_0^z a(\tau, z') dz' \right]$$

vs the altitude of the source z in km for $\tau = 10$ sec, 30 sec and 100 sec, where the scale height H is assumed to be 8 km.

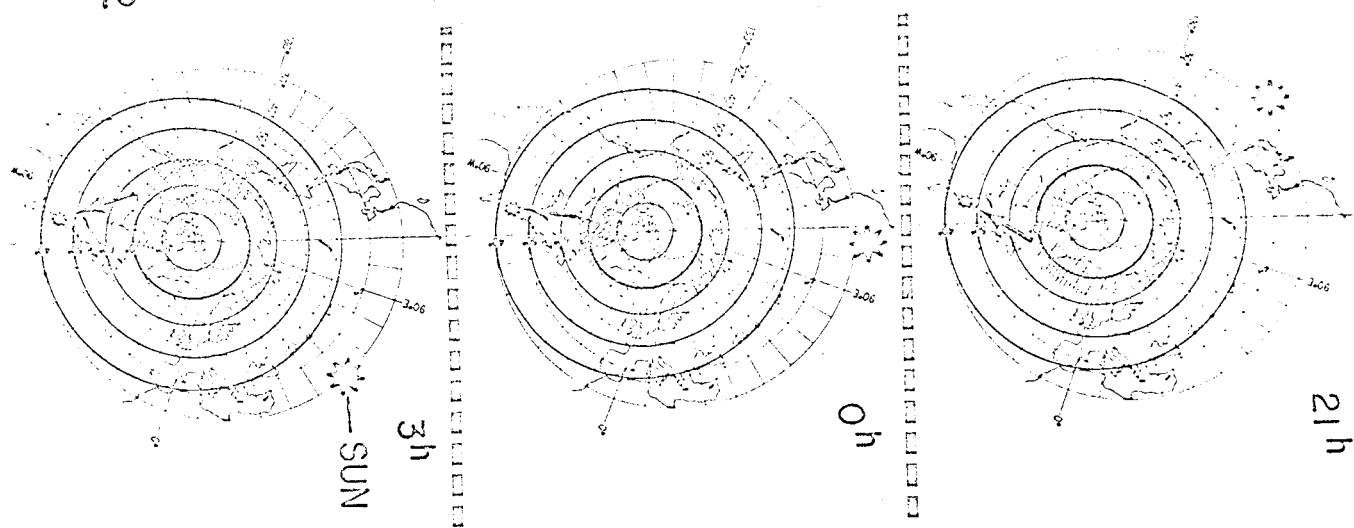
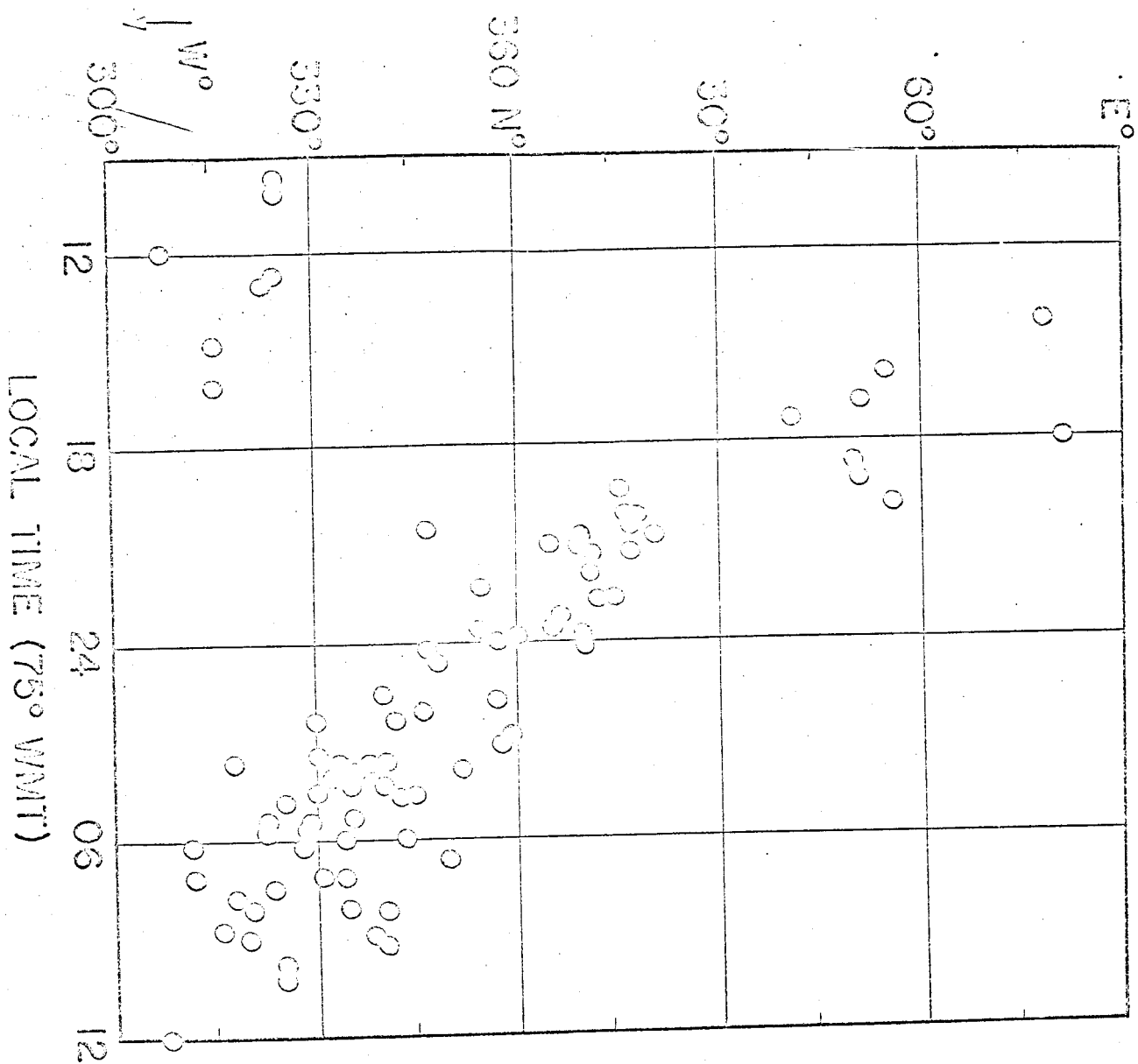


Fig. 3

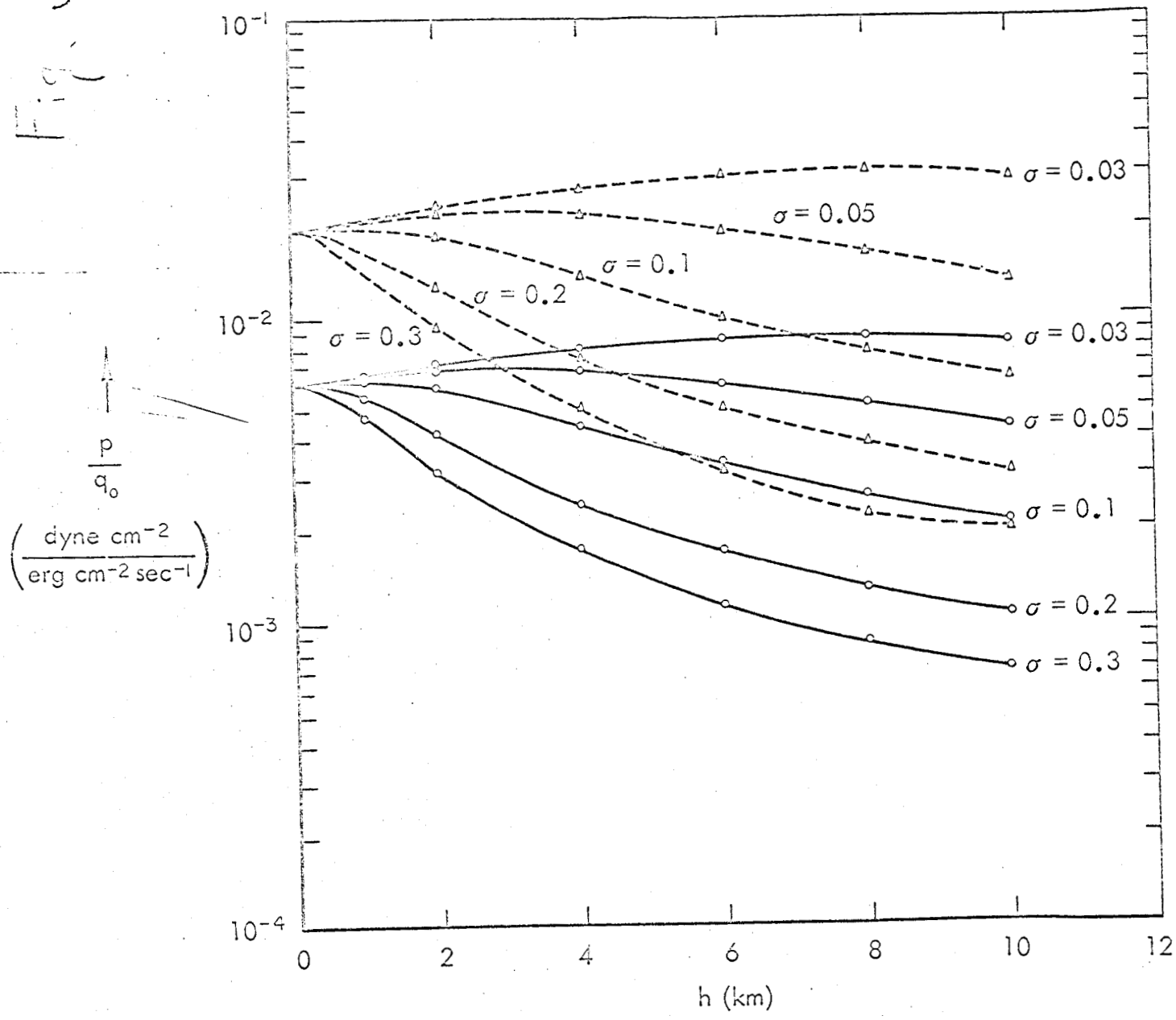
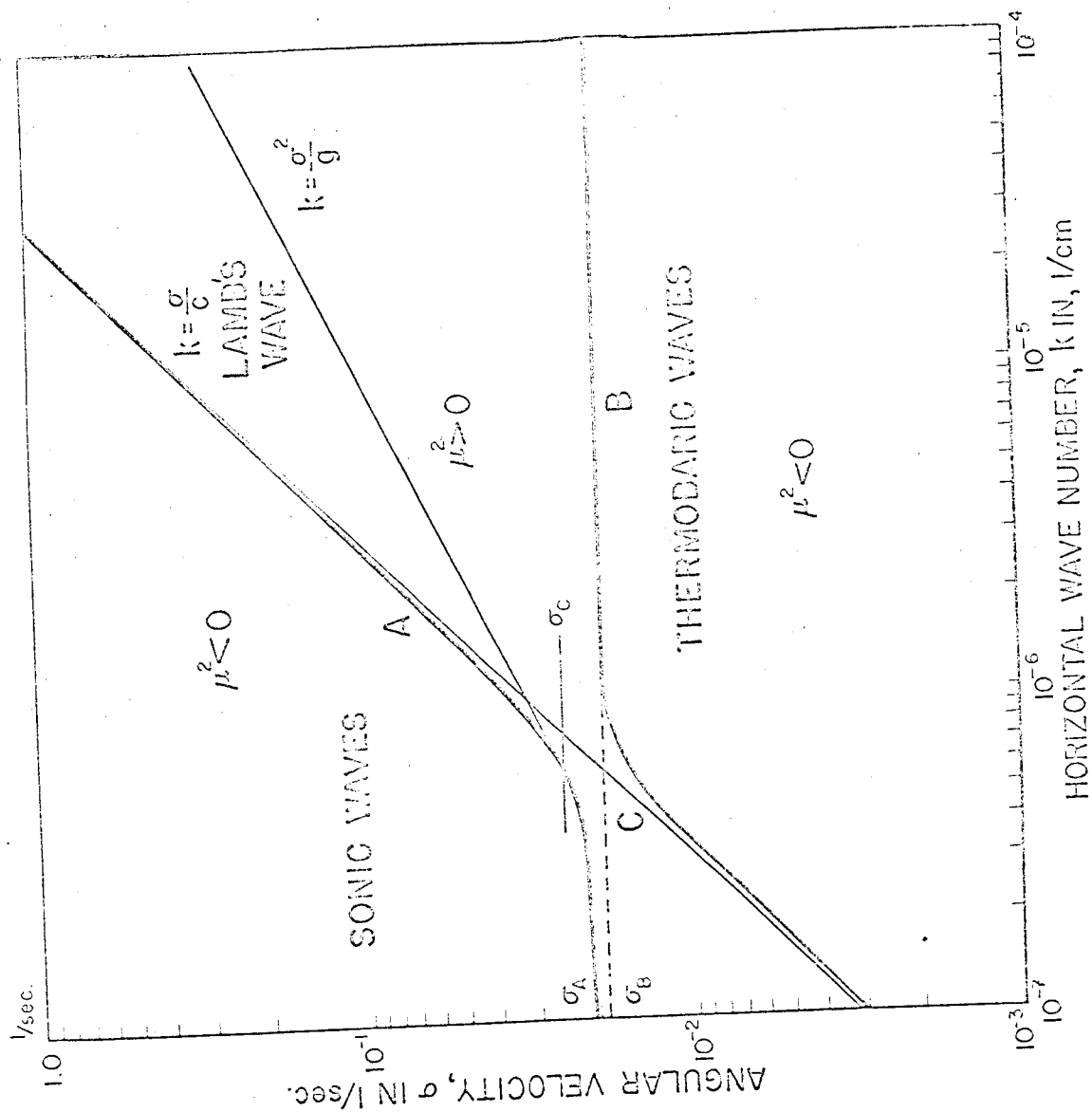


Fig. 4



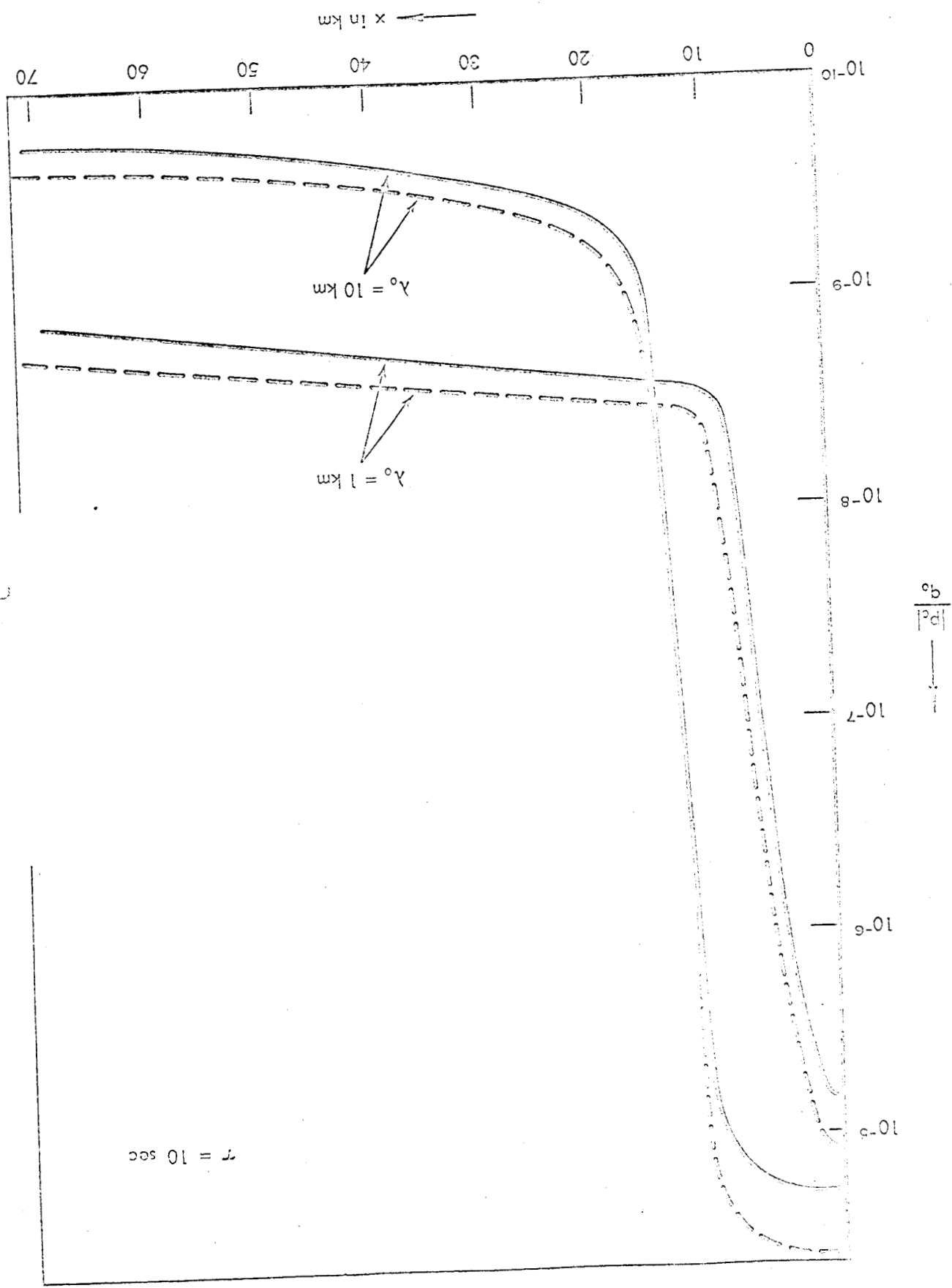
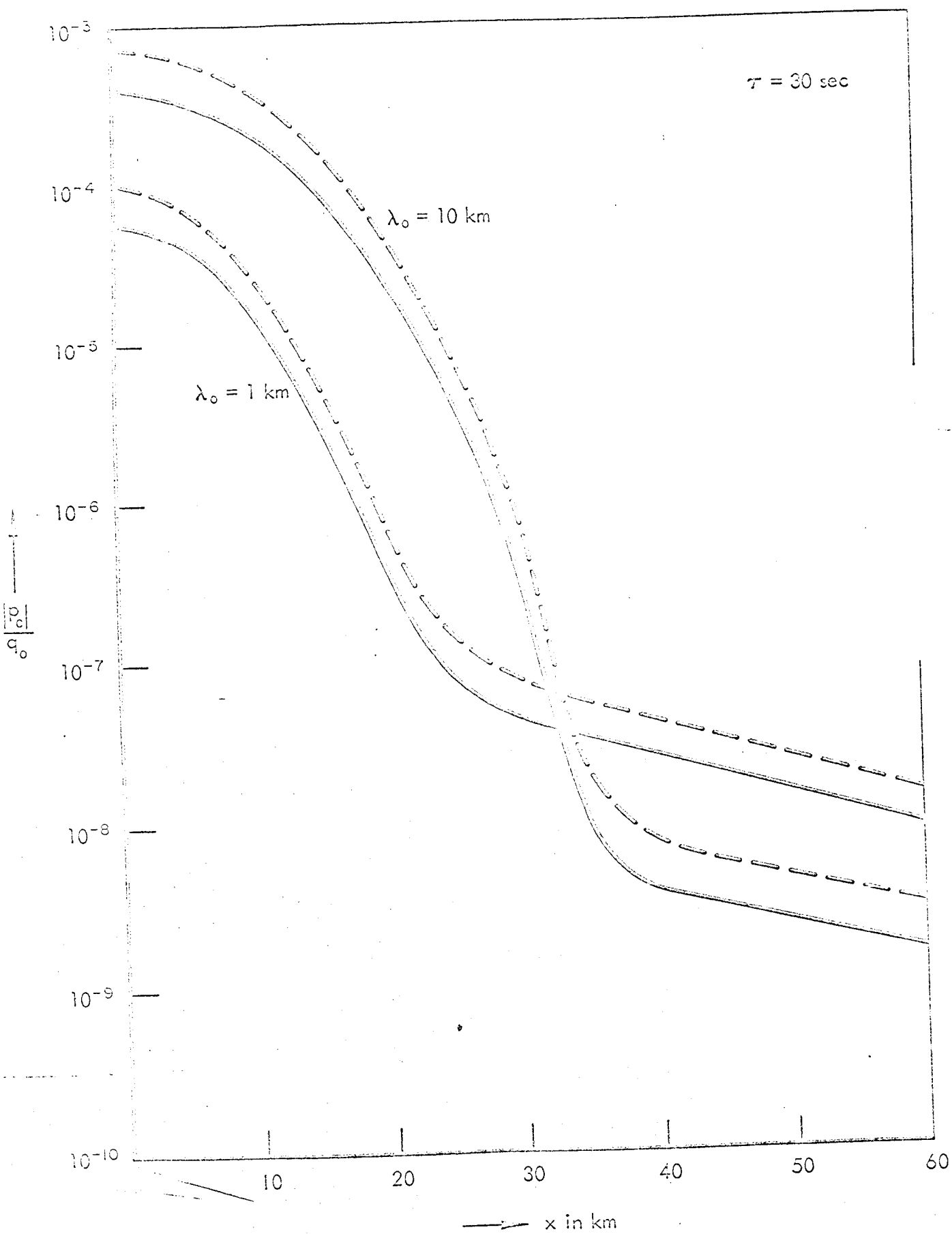
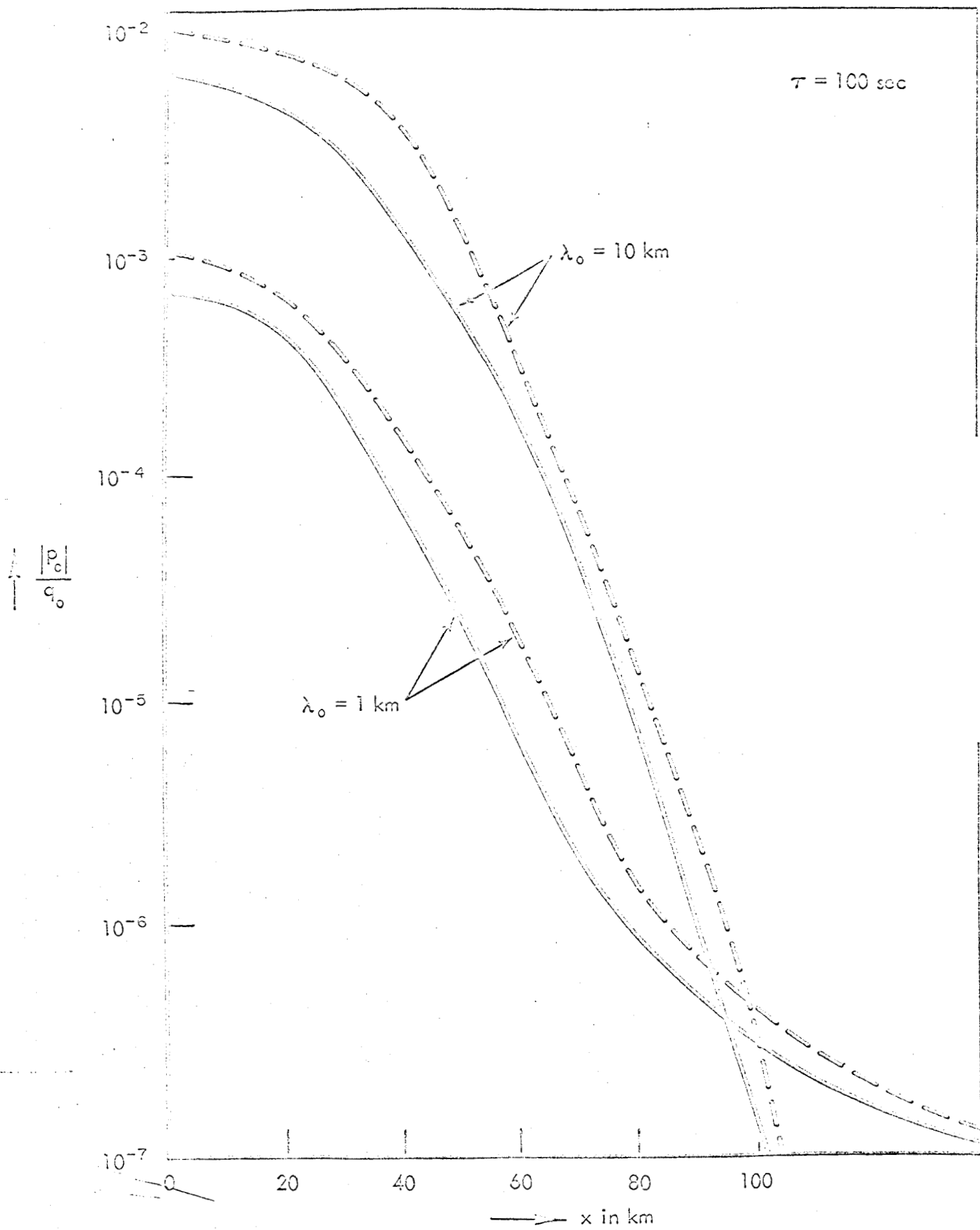
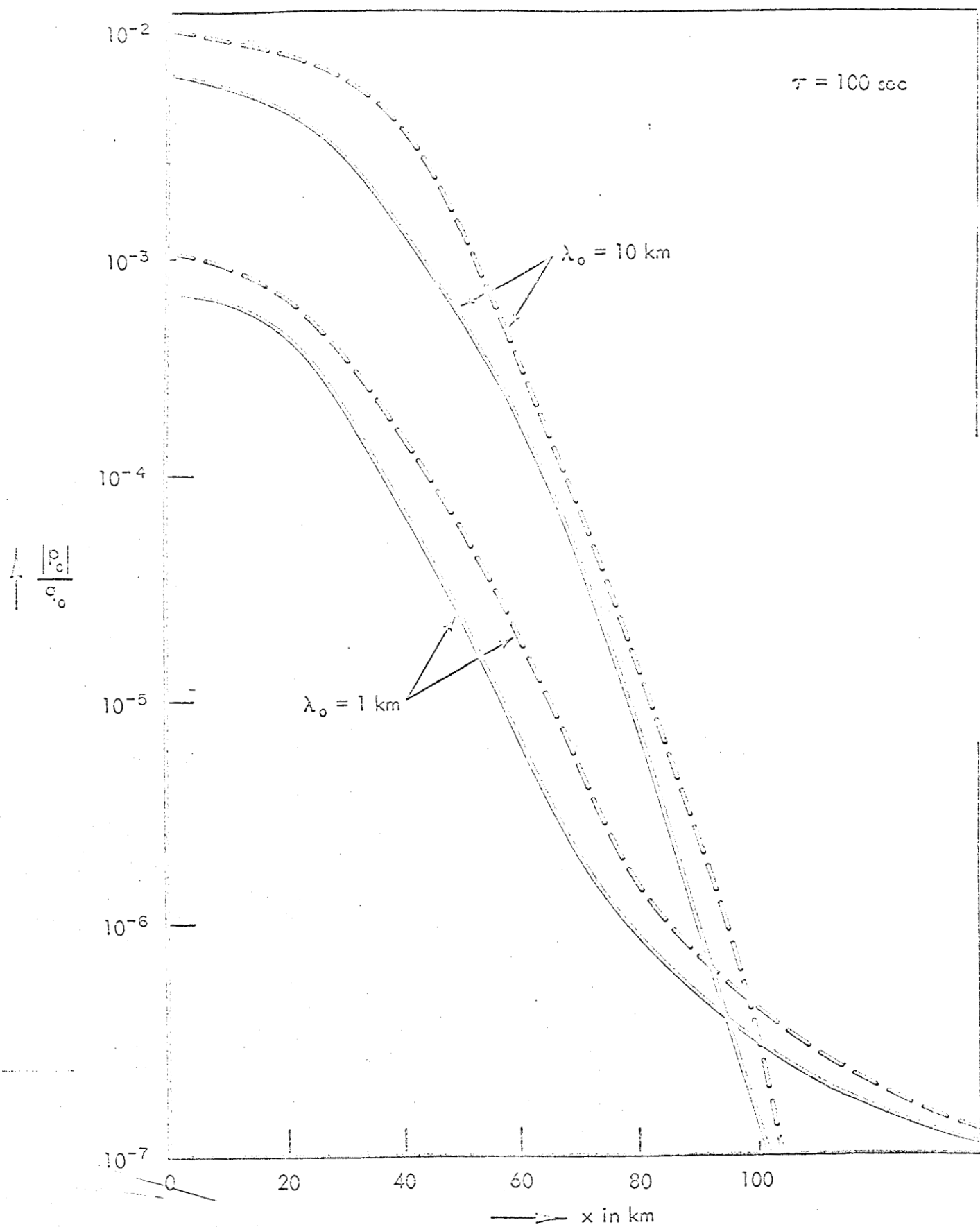


Fig. 10

$\tau = 10 \text{ sec}$







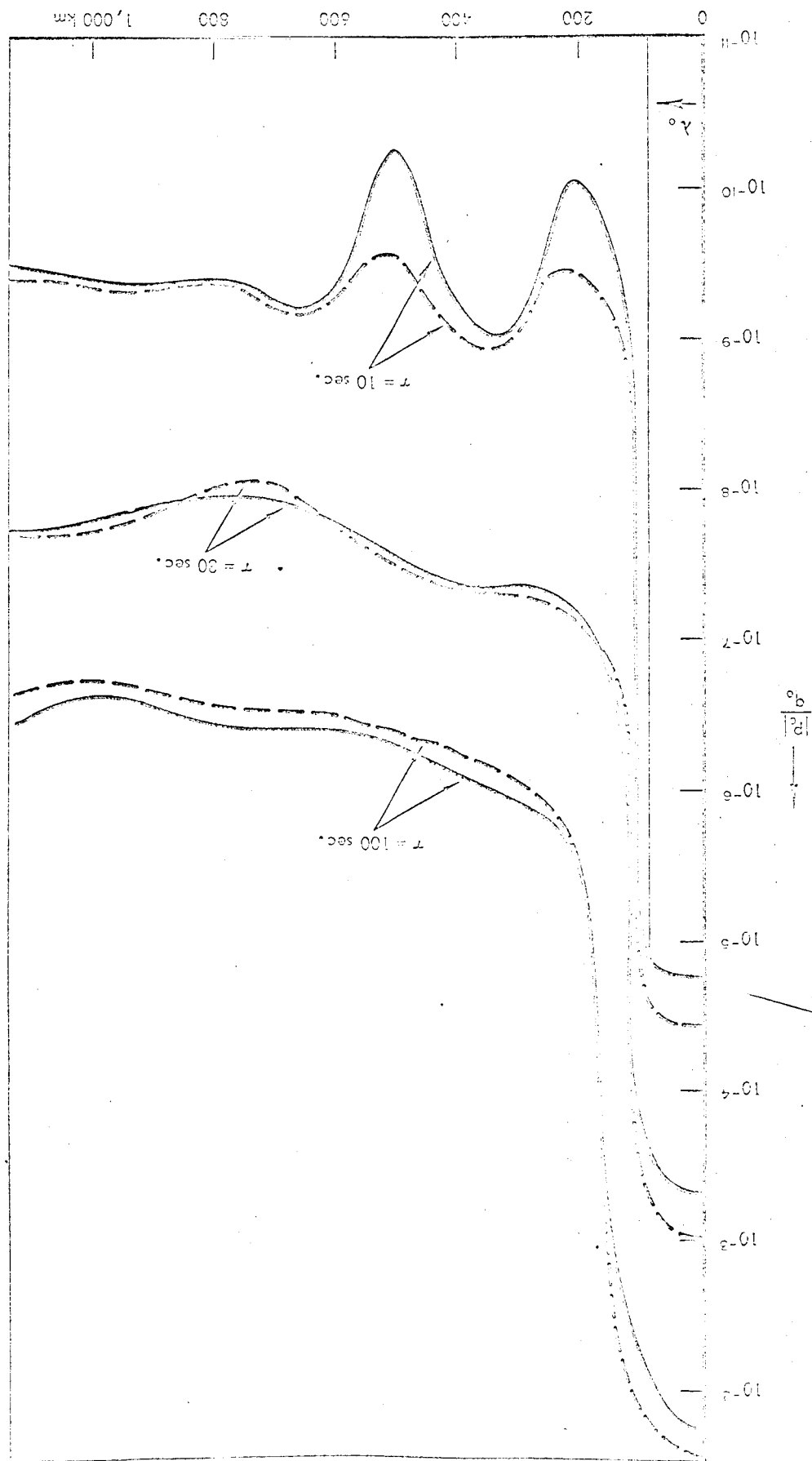


Fig. 6

